Counting Photons to Calibrate a Photometer for Stellar Intensity Interferometry

A Senior Project

Presented to the Department of Physics

California Polytechnic State University, San Luis Obispo

In Partial Fulfillment

of the Requirements for the Degree

Bachelor of Science

By Jason Chew

July, 2013

Advisor, Dr. Jodi Christiansen

Abstract

We use a telescope and photometer to observe stellar photons and measure the rate of observed photons. Based on intensity spectra from the Spectrophotometric Catalogue of Stars, we also predict expected values for the photon rates, which we compare to our measurements. From this comparison, we measure the local optical depth to be $\tau = 0.60 \pm 0.25$, a reasonable value. We find that our predictions are directly proportional to our measurements by a factor of $0.98^{+0.02}_{-0.27}$. The similarity between our measurements and expectations shows that we are able to both predict and measure photon rates with accuracy.

Introduction

Stellar intensity interferometry (SII) uses the correlations between the observations of multiple telescopes to measure the diameter of a star and to observe small features of a star. In our experiment, we use a photometers that we constructed and a telescope on Cal Poly's campus to make such observations. The main purpose of our experiment is to develop methods by which we can consistently predict and methods by which we can consistently measure photon rates from stars.

We develop a process for measuring the number of photons observed from the raw voltage data, taken with a telescope that is available to us on Cal Poly's campus and a photometer that we constructed ourselves. We use these measurements to determine the optical depth of the atmosphere. By using the optical depth as a parameter, we predict photon rates for various stars. These predictions are consistent with our measurements, though the error bars are larger than is preferable. We theorize that uncertainty in measurements is dominated by atmospheric conditions.

In the future, we plan to repeat our measurements with more consistent atmospheric conditions. The analytic methods that we develop can be applied to larger telescope arrays. The Cherenkov telescope array, for example, is comprised of 61 telescopes. Though its intended purpose is to image photon cascades from gamma rays, by observing stars, the array could be used for SII.

PMT and Photon Counting Statistics

The Cal Poly telescope gathers light from a star through its 12” aperture. The light is then focused by a series of mirrors and lenses to the location of the eyepiece where we have placed a photometer. The photometer consists of a fabry lens, a B-440 blue Edmund light filter, and a photomultiplier tube (PMT), which is powered with an external high voltage source. However, before affixing the photometer to the telescope, we used an indoor setup in a darkroom for initial calibrations with the

PMT. The PMT was encased in a sealed metal tube with a pinhole aperture on the front, as shown in Figure 1. We adjusted the amount of light incident on the PMT by shutting off lights inside the room and opening the door to various angles. We used the data samples from this indoor setup to find optimal settings for the high voltage power source.

A PMT consists of a photocathode and a series of dynodes at increasing electric potentials. When a blue photon enters the PMT, it hits the photocathode with some probability of causing the emission of an electron by the photoelectric effect. If an electron is emitted in this way, it goes to the first dynode, causing the emission of multiple electrons. Each of these new electrons flow down the tube from dynode to dynode, creating more electrons at each stage. At the end of the PMT, the cascade of electrons runs through a resistor, whose voltage we observe. Thus every photon that causes the emission of an electron produces a voltage spike. This voltage signal is amplified upon leaving the PMT and is then recorded by an oscilloscope. Outside of the detection of a photon by this process, the output signal is simply a collection of electronic noise.

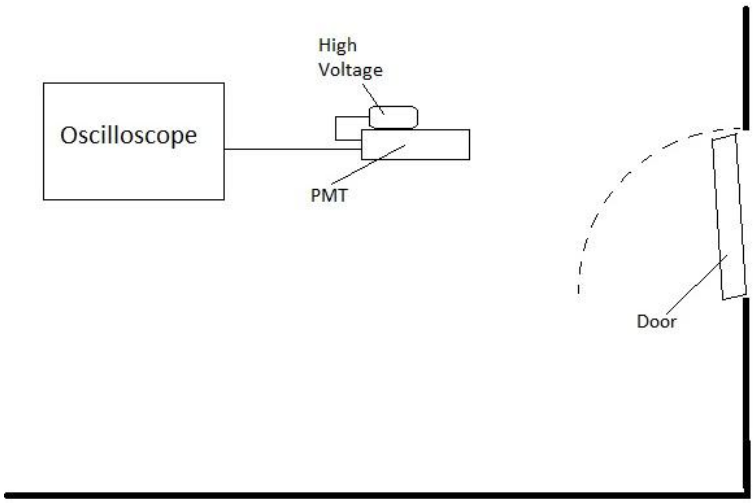

Figure 1: Indoor lab setup

The raw data that we obtain is an array of output voltages taken during the collection time of 2ms. This is organized into a plot of voltage versus time. Figure 2 shows voltage pulses in red which correspond to the observation of a photon, using data taken observing Castor. Determining the parts of the plot that we think are moments of darkness (no photons) and the parts that we think are instances of the detection of a photon is crucial to being able to discuss statistical aspects of the photons. A simple way to differentiate between darkness and photon detection is to set a threshold voltage that a pulse must surpass in order to be considered a photon. We consider all data points above the threshold and points near them to be one or more photons.

Data not selected as a photon are said to be "dark". As shown in Figure 2 in black, the voltages at these points oscillate about a constant voltage due to electronic noise. The mean of the voltage of all these dark points is the offset voltage, shown as a green line in Figure 2. For simplicity of calculations, we subtract the offset voltage from the entire dataset to calculate the areas of the photon pulses in a simple way.

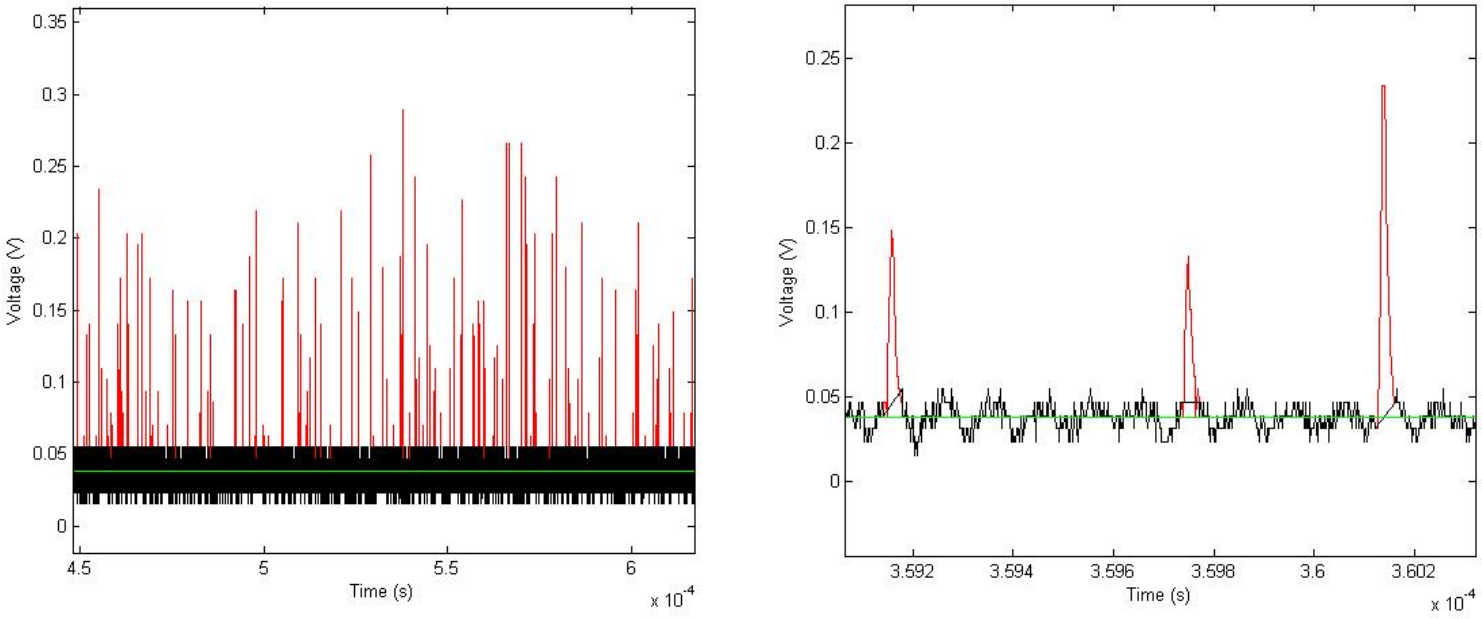

Figure 2: Voltage readouts: over 0.15μs (left) and over 10ns (right)

Using Reimann sums, we calculate the area of each individual pulse and store them in an array. When this collection of areas is organized into a histogram, the pattern shown in Figure 3 emerges. For a low intensity light source, the likelihood of multiple photons being observed at the same time is extremely low. Thus, the statistical spread of the areas is a single Gaussian as shown in Figure 3. We use MATLAB to fit the data from the histogram to the equation

$$G(x) = a_1 e^{\frac{-(x-b)^2}{2c^2}} \tag{1}$$

where a_1 is the height of the distribution, b is the location of the center, and c is the full-width, half-maximum value.

Notice that we observe a large number of pulses with a very small area relative to other areas. These pulses are caused by electronic noise that was not filtered out by our threshold voltage. This is an indication that our threshold value was well-chosen. We know that no photon pulses are missed, because some of the small noise pulses are still counted. Therefore, the threshold is not set too high. Furthermore, since we are able to clearly identify and account for noise pulses, the threshold is not set too low.

As Figure 3 indicates, there is a significant portion of the Gaussian distribution whose x-value is less than zero. If this were not the case, the central position of this Gaussian (with units in Vns) would be considered the average area due to a single photon. However, the portion of the distribution left of x = 0 does not correspond to any real measurement because it would correspond to nonexistent negative areas. While the center of the Gaussian is located at b = 1.1 Vns, the average area of a single photon is p_1 = 1.3 Vns. The width of the Gaussian is described by the value c = 0.9 Vns.

The number of photons in Gaussians corresponding to the detection of a single photon is

$$N_1 = \frac{\int_0^{\infty} a_1 e^{\frac{-(x-b)^2}{2c^2}}}{p_1} \tag{2}$$

In Figure 3, we used data taken when looking at Gemini Kappa and measured N_1 = 1309±36. Figure 4 shows the data taken with the indoor setup for a high intensity light source with multiple Gaussians fit to the histogram data. The black curves are individual Gaussian distributions and the red curve is their sum. For higher intensity sources, there is a significant chance that photon pulses may overlap, causing a single pulse of a larger area rather than multiple smaller pulses. The histogram for such high intensity sources is modeled as a sum of multiple Gaussian distributions, each representing a distribution of one, two, three, etc. overlapping photons.

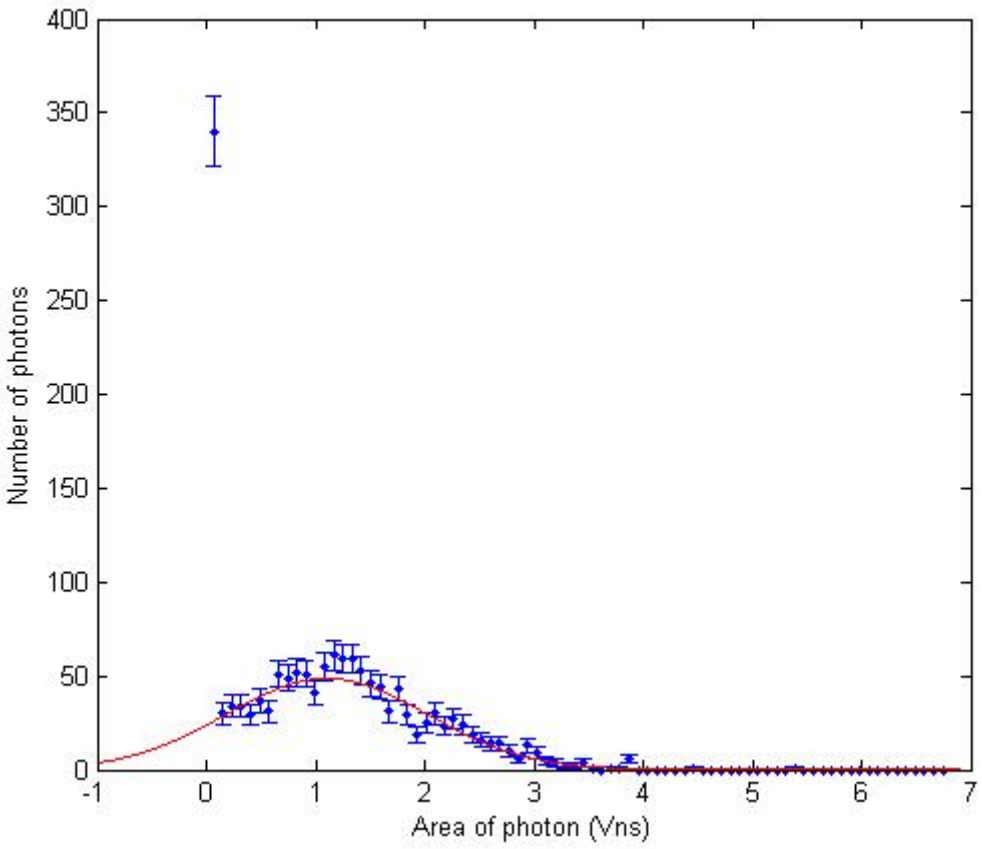

Figure 3: Gaussian distribution for the detection of single photons

Unlike the single photon distribution, the mean value of pulses representing multiple photons is the center of their Gaussian distributions. Once we have determined values for the mean area of photon pulses, we determine the total number of photons observed. The number of photons in every Gaussian excluding the first is

$$N_{mult} = \frac{A_{tot} - N_1 p_1}{b} \tag{3}$$

where A_{tot} is the total area above the offset voltage.

The total number of observed photons is therefore $N_{tot} = N_1 + N_{mult}$. The precision with which our fitted Gaussian functions match the data is an indication that our photon counting is accurate. In Figure 4, we used the indoor setup, with relatively high intensity light for our source. For the data represented in Figure 4, $N_1 = 1380 \pm 40$, $N_{mult} = 46350 \pm 220$, and $N_{tot} = 47730 \pm 220$.

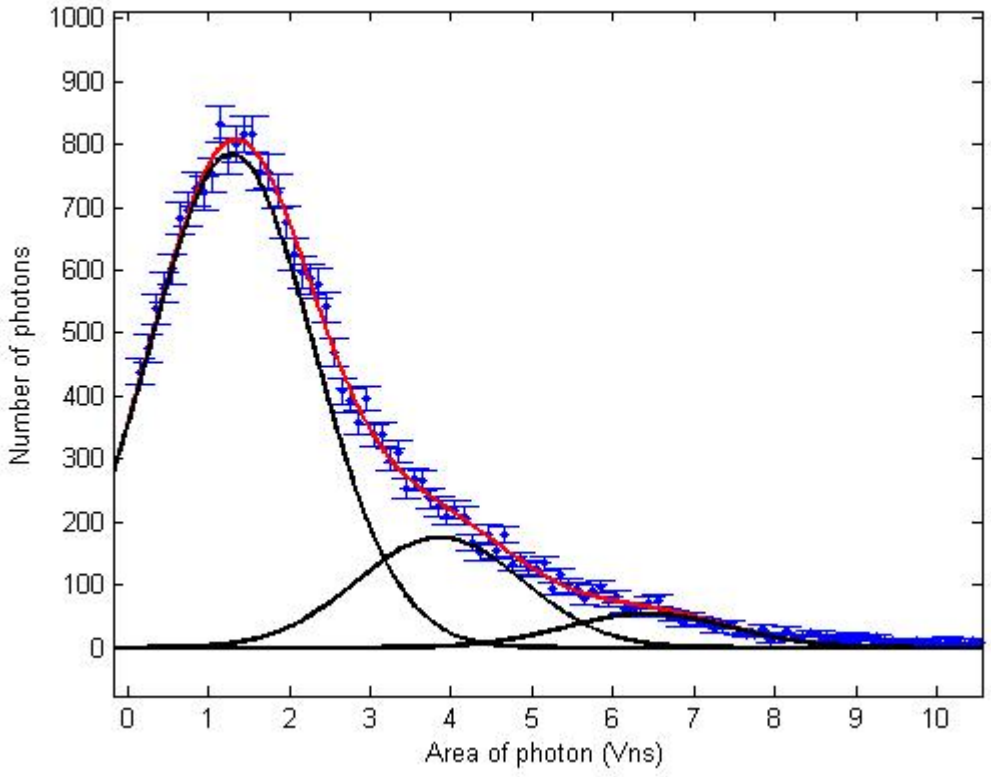

Figure 4: Gaussian distributions for a high intensity source

Predicted Photon Rates

To draw conclusions from the measured photon rates, we compare them to predicted rates for a given star. We predict photon rates as accurately as possible outside experimentation by taking into account the magnitude of the star, the spectrum of the star, the size of the telescope, the efficiency of our various optical instruments, and the quantum efficiency of the PMT itself. Many of these efficiencies are wavelength dependent.

In predicting the rate of observed photons for a given star, we start with its brightness. The Spectrophotometric Catalogue of Stars[1] has a database containing the flux rates for all the stars that we observed as well as many others. The fluxes of stars ($mW/m^2/cm$) are given as a function of wavelength. The product of these rates with the efficiency of the Edmund blue filter we use gives the intensity transmitted to the PMT. The efficiency of the PMT itself is also dependent on the wavelength of incident light. Thus, we multiply the PMT's efficiency spectrum into the flux rates as well. Each of these separate wavelength-dependent efficiencies and the resultant overall spectrum observed by the PMT are shown in Figure 5.

By multiplying the combined spectrum by the area (A_{tel}) of the aperture of the telescope we find the transmitted power at each wavelength. Consider photons with a small range of wavelengths ($\Delta\lambda$) near some central wavelength λ_0. If the intensity of such photons is I, then the rate of photons per unit area is

$$N(\lambda_0) = \frac{A\, I(\lambda_0)}{E_{photon}} \quad . \tag{4}$$

Because the energy of a photon is inversely proportional to its wavelength, the photon rate can also be described as

$$N(\lambda_0) = \frac{A\, I(\lambda_0)}{hc}\lambda_0 \quad . \tag{5}$$

In order to obtain the overall photon rate for all wavelengths, we form this equation into an integral. The integral

$$N = A_{tel} \int_0^{\infty} I_{star}(\lambda)\epsilon_b(\lambda)\epsilon_{atm}(\lambda)\epsilon_{PMT}(\lambda)\, d\lambda \tag{6}$$

gives our prediction of the rate of observed photons from a star accounting for the aforementioned efficiencies. A_{tel} is the area of the telescope, ε_b is the efficiency of the blue filter, ε_{atm} is the efficiency of the atmosphere, and ε_{PMT} is the quantum efficiency of the PMT. Table 1 contains a list of stars, their measured photon rates, their predicted photon rates with and without accounting for optical depth, and their altitudes. Since all of our data samples are taken over the course of 2ms, these predicted photon rates are given as the predicted number of photons in a 2ms interval in Table 1.

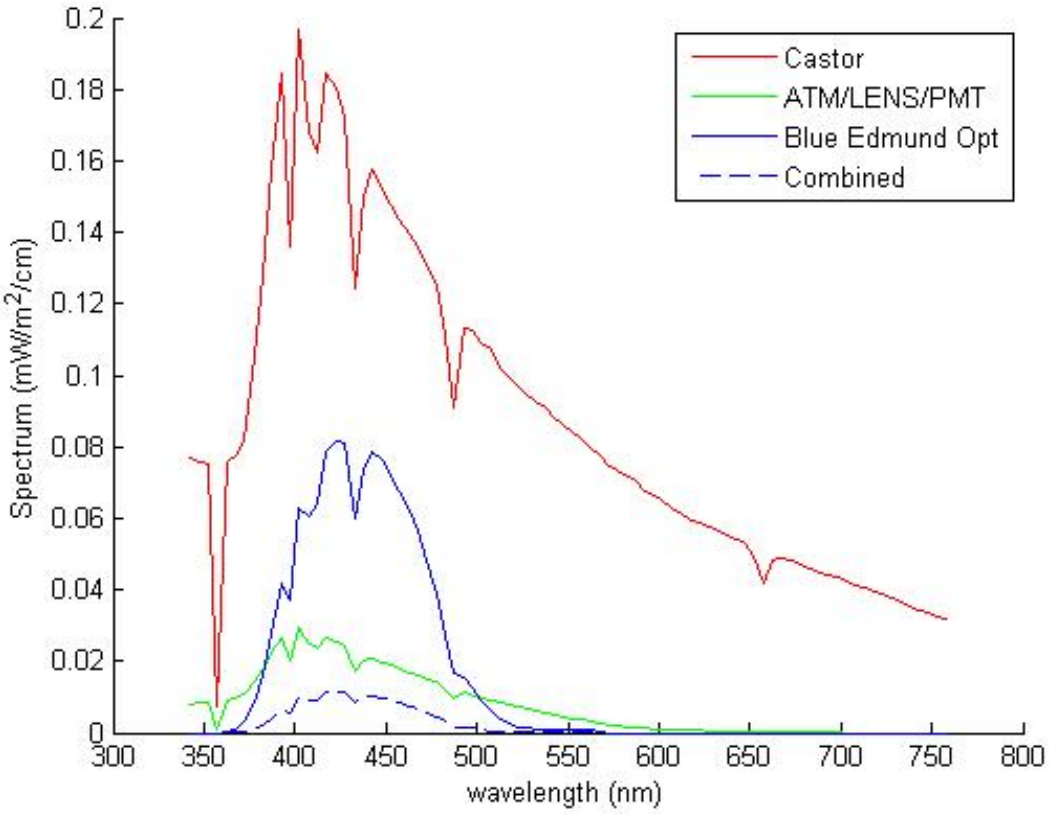

Figure 5: Efficiencies and overall energy spectrum

Optical Depth

Notably, the attenuation of light by the atmosphere have not yet been factored into our predictions. The optical depth that characterizes this attenuation is highly dependent on local factors. Because there are not observatories that have taken reliable measurements concerning optical depth, we measure this value experimentally by comparing our predictions to the measured photon rates at various altitudes. The intensity, *I*, as a function of the altitude of the star is

$$I = I_0 e^{\frac{-\tau}{\sin\theta}} . \quad (7)$$

I_0 is the intensity of light without atmospheric effects, τ is the optical depth, and θ is the altitude of the star. Since the number of incident photons is proportional to the intensity of light, the relationship between the number of photons we observe and the number of photons we predict without accounting for atmosphere is

$$N_{obs} = A_0 N_{pred} e^{\frac{-\tau}{\sin\theta}} . \quad (8)$$

Arranging the equation in this linear form

$$\ln\left(\frac{N_{obs}}{N_{pred}}\right) = \ln(A_0) - \tau \frac{1}{\sin\theta} \quad (9)$$

produces a better fit. A_0 is a proportionality constant that accounts for the unknown efficiency of lenses and mirrors within the telescope.

Target	Altitude (Degrees)	Predicted Counts (without optical depth)	Predicted Counts (with optical depth)	Measured Counts (Counting error)
Castor	62.9	27314	13922	14000±120
Capella	48.3	54570	24434	24743±160
Auriga Beta	54.4	21244	10154	9466±97
Auriga Delta	52.8	1451	683	1220±35
Gemini Theta	59.3	3884	1933	2273±48
Gemini Kappa	63.6	1891	968	1465±38
Pollux	66.7	16773	8725	9332±97

Table 1: Targets, predictions, and measurements

To find the optical depth, we used data taken on a single night of several different stars at various altitudes. We plot the natural log of the ratio of measured to predicted photon rates versus the reciprocal of the sine of the altitude of the star, as shown in Figure 6. By using a weighted fit for the linearized equation, we measure the optical depth to be $\tau = 0.60 \pm 0.25$.

The relatively large uncertainty in this value is due to the wide variance in the number of counted photons. If two data sets are taken of the same star, one directly after the other, we find that the number of observed photons vary by as much as twenty percent. This effect is shown visually in Figure 6, the data points come in pairs that are two measurements of the same star with one measurement directly before the other. For many of these pairs, the gap between them is relatively large by comparison to the

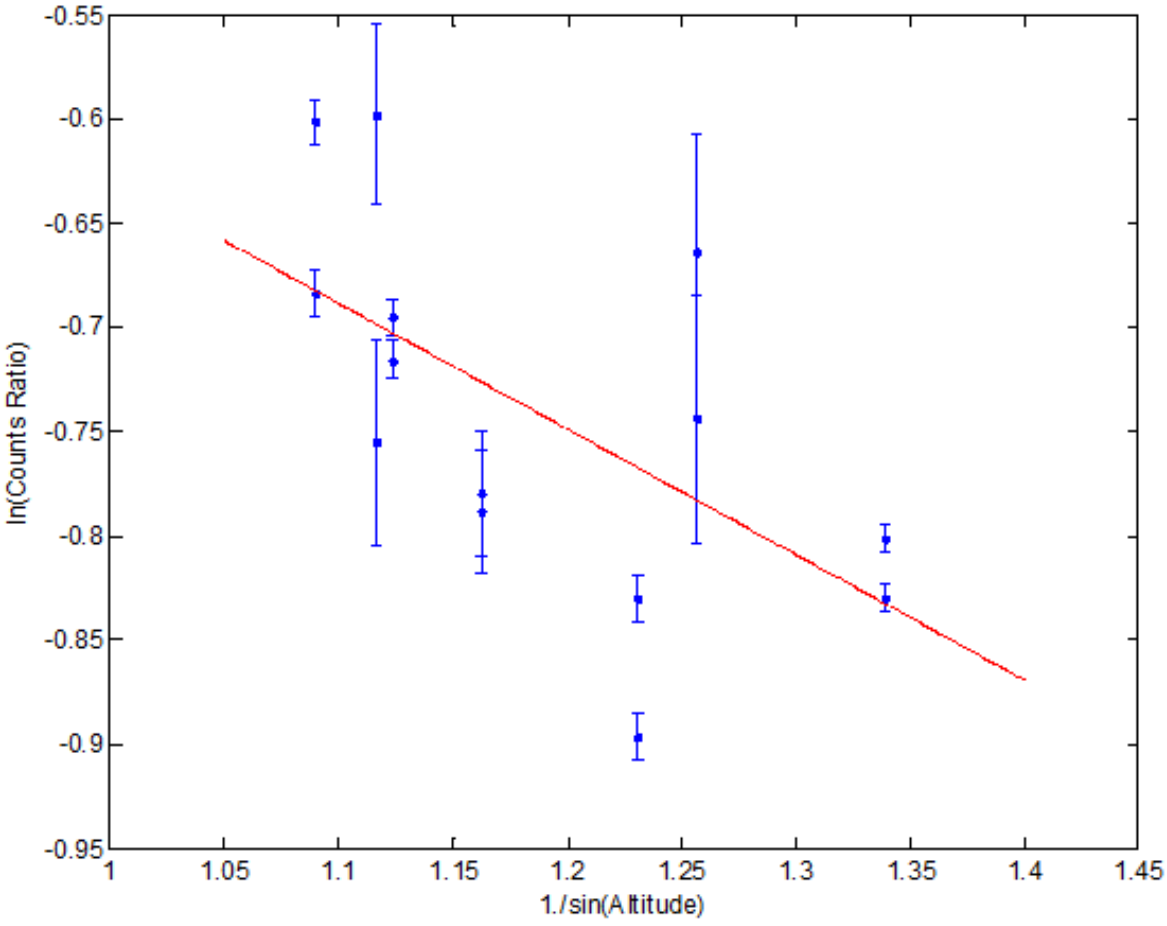

Figure 6: Linearized plot for finding optical depth

Poisson uncertainty from counting. The suddenness with which the measured photon rates change leads us to think that the variance is due to random atmospheric effects.

In Figure 6, the errorbars on the data points are the counting errors associated with the rates. The majority of the data points are not consistent with the fitted line according to these errorbars. However, taking into account that the observed photon rates vary somewhat widely, we can see that the fit line appears to be consistent with the data. For many of the data set pairs, the line goes directly between them. For the other data set pairs, the separation between the data points and the fitted line is less than or approximately equal to the separation between the two points. Correlation is high between our predictions and measurements.

Calibration Constant, A_0

The linear behavior of the data in Figure 6 shows that the measured and predicted counts are proportional to one another. Using the optical depth found in with the fitted line, we calculate the predicted counts, accounting for atmospheric attenuation. Figure 7 shows the plot of measured counts versus predicted counts. We fit these data points to a line as well, but we set the y-intercept at zero because the predicted and measured counts should be directly proportional. The slope of this line is the constant of proportionality between our predicted and measured counts referred to earlier as A_0, and we measure it to be $0.98^{+0.02}_{-0.27}$. This value is very close to 1, indicating that our predictions are very close to our measured values within errorbars.

Conclusions

We compared our measured data for the photon rates of stars to our predictions and from their ratio calculated the optical depth $\tau = 0.60 \pm 0.25$. The uncertainty in this result is dominated by the variance

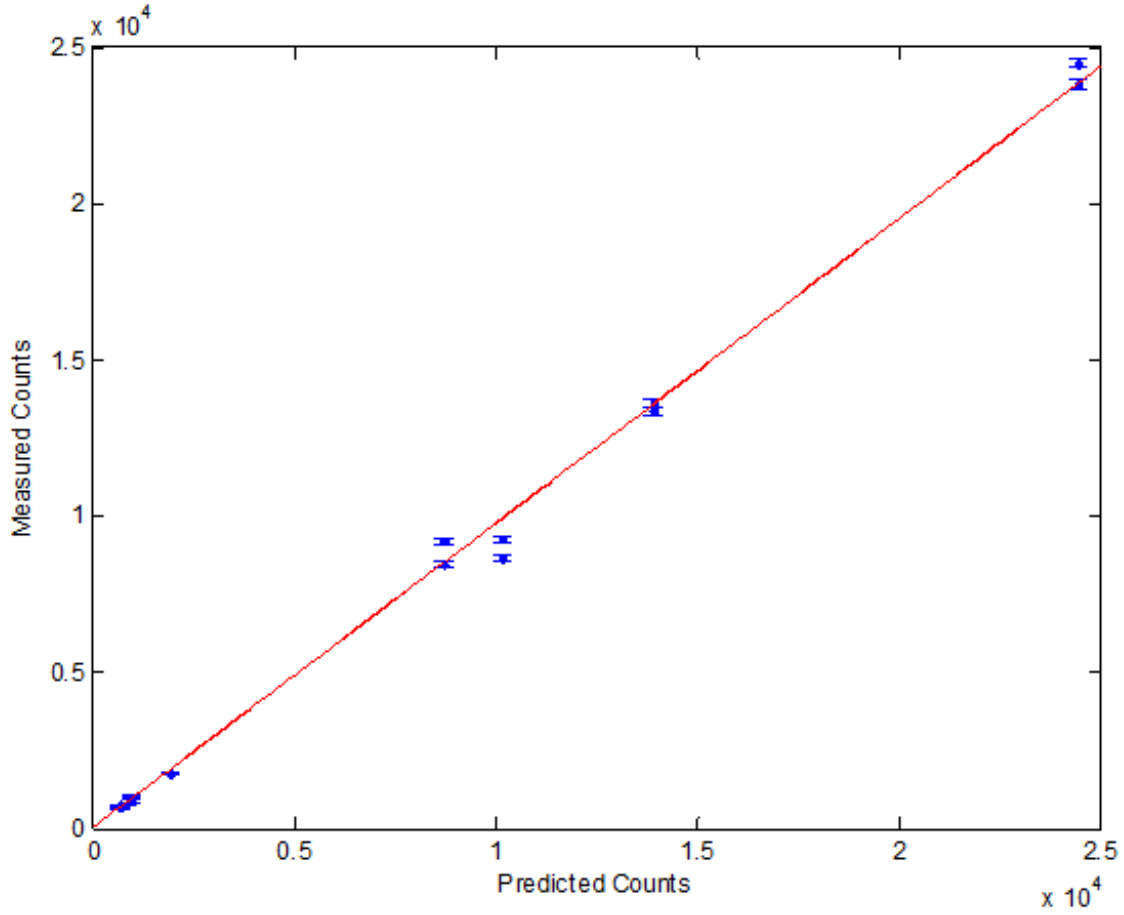

Figure 7: Measured versus predicted with optical depth

in observed photons during measurement. Because our individual data sets consistently follow expected statistical patterns, we believe that this spread indicates that the rate of photons incident on the detector is itself inconsistent. A likely cause for this is local atmospheric effects having a significant effect on the incident rate of photons. After accounting for atmospheric attenuation, the fitted constant of proportionality between our measurements and our predictions is $0.98^{+0.02}_{-0.27}$. This small difference between our measurements and predictions suggests that our methods for both are consistent.

References

1. Kharitonov, A.V., Tereshchenko, V.M., and Knyazeva, L.N., 1997. Spectrophotometric Catalogue of Stars. VizieR Online Data Catalog III/202